JETIR.ORG ISSN: 2349-5162 | ESTD Year : 2014 | Monthly Issue
JOURNAL OF EMERGING TECHNOLOGIES AND INNOVATIVE RESEARCH (JETIR)
An International Scholarly Open Access, Peer-reviewed, Refereed Journal

MATHEMATICAL MODELING OF THE EPIDEMIC CONTROL MEASURES IN OVERCOMING COVID-19 OUTBREAKS

Dr.S.Kalaiselvi,
PG & Research Department of Mathematics,
The Standard Fireworks Rajaratnam College for women (Autonomous), ,
Sivakasi,VirudhuNagar,TamilNadu, India

Abstract : **This study investigates the role of vaccination, quarantine, and isolation in controlling the spread of COVID-19 using a homotopy perturbation method.**

IndexTerms **- Vaccination, quarantined, isolation.**

I. INTRODUCTION

Mathematical modeling has become an essential tool in understanding the transmission dynamics of infectious diseases, particularly during global outbreaks such as COVID-19[1,2]. It provides a structured framework to analyze how diseases spread within a population and to evaluate the effectiveness of various control strategies.

In this study, the total population is categorized into different compartments, namely susceptible, exposed, vaccinated, quarantined, infected, and recovered individuals[2,3]. The interactions among these compartments are described through a system of nonlinear differential equations, which capture the complex nature of disease transmission[4,5].

Due to the nonlinear structure of the model, obtaining exact analytical solutions is often difficult. Therefore, the Homotopy Perturbation Method (HPM) is employed to derive approximate analytical solutions[6,7,8]. In addition, numerical simulations are carried out using MATLAB to validate the analytical findings and to examine the influence of key epidemiological parameters.

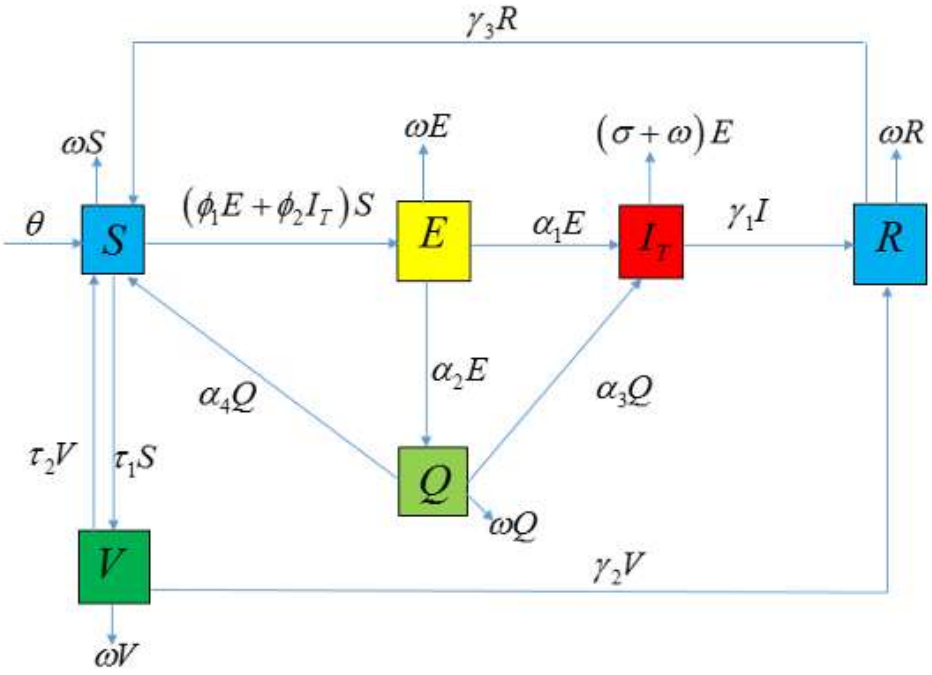
The primary objective of this work is to investigate the spread of COVID-19 and to assess the impact of control measures such as vaccination, quarantine, and treatment. The outcomes of this study contribute to a better understanding of disease dynamics and support the development of effective public health intervention strategies.

II Mathematical Model Formulation:

In this current study, we propose a deterministic $SEVQI_TR$ model for the transmission dynamics and control of COVID-19. We divide the total human population into six compartments:

- **Susceptible (S):** Individuals who are healthy but at risk of contracting the virus. This population increases through the recruitment rate (θ), individuals losing immunity after recovery (γ_3), and those whose vaccine-induced immunity has waned (τ_2).
- **Exposed (E):** Individuals who have been infected with the virus but are not yet fully infectious or showing severe symptom. They progress into this class through contact with infected individuals.

- **Vaccinated (V):** Individuals who have received a COVID-19 vaccine. This class increases as susceptible people are vaccinated at a rate τ_1.
- **Infected but Isolated (I_T):** Confirmed cases that are isolated in treatment centers. This compartment includes infectious individuals from both the exposed and quarantined group.
- **Recovered (R):** Individuals who have successfully recovered after treatment in isolation or who have achieved immunity through vaccination[9,10].



Equations

The Model for COVID-19 Disease dynamics can be represented by

$$\frac{dS}{dt} = \theta - (\phi_1 E + \phi_2 I_T)S + \alpha_4 Q + \tau_2 V + \gamma_3 R - (\tau_1 + \omega)S \quad (2.1)$$

$$\frac{dE}{dt} = (\phi_1 E + \phi_2 I_T)S - (\alpha_1 + \alpha_2 + \omega)E \quad (2.2)$$

$$\frac{dV}{dt} = \tau_1 S - (\tau_2 + \gamma_2 + \omega)V \quad (2.3)$$

$$\frac{dQ}{dt} = \alpha_2 E - (\alpha_3 + \alpha_4 + \omega)Q \quad (2.4)$$

$$\frac{dI_T}{dt} = \alpha_1 E + \alpha_3 Q - (\gamma_1 + \delta + \omega)I_T \quad (2.5)$$

$$\frac{dR}{dt} = \gamma_1 I_T + \gamma_2 V - (\gamma_3 + \omega)R \quad (2.6)$$

Simulation and Analysis of Disease Transmission Dynamics Using HPM

The present study is based on a nonlinear epidemic transmission model that was originally developed using fractional-order differential equations to describe the spread of infectious diseases. In the reference research work, the population dynamics were analyzed by incorporating important epidemiological control measures such as vaccination, quarantine, isolation, and treatment. The fractional modelling framework was adopted to capture the memory-dependent characteristics of disease transmission, thereby providing a more realistic representation of epidemic progression. The authors of the original study investigated the qualitative properties of the model by establishing the existence and uniqueness of solutions and by examining stability behaviour through appropriate fixed point theoretical approaches. Numerical simulations were also performed to illustrate how variations in transmission and recovery parameters influence infection levels within the population.

In the present work, the same nonlinear epidemic structure has been reformulated into a system of ordinary differential equations in order to obtain a clearer analytical understanding of the disease dynamics. This reformulation simplifies the mathematical complexity associated with fractional derivatives while preserving the essential interactions among different epidemiological compartments. Since the resulting nonlinear coupled system does not admit an exact closed-form solution, an approximate analytical technique is required to analyze the temporal behaviour of the model variables.

To overcome this limitation, the Homotopy Perturbation Method has been applied to derive a semi-analytical solution in the form of a convergent series expansion. This method effectively decomposes the nonlinear terms and enables a systematic investigation of the variation of susceptible, exposed, infected, and recovered populations with respect to time. The analytical expressions obtained through the HPM approach provide useful insight into the influence of epidemiological parameters on disease propagation and control.

Furthermore, the approximate analytical solutions have been validated through numerical simulations carried out using MATLAB. Graphical representations obtained from the computational analysis demonstrate the significant role of increased vaccination coverage, timely quarantine measure, and effective treatment strategies in reducing the spread of infection. Thus, the combined analytical reformulation, semi-analytical solution technique, and numerical simulation provide a comprehensive understanding of nonlinear epidemics and contribute to the development of efficient disease control policies.

In conclusion, the combined analytical reformulation of the fractional epidemic model into an ordinary differential equation framework, together with the application of the Homotopy Perturbation Method and MATLAB-based numerical validation, provides a comprehensive understanding of nonlinear disease transmission dynamics. The study emphasizes the importance of mathematical modelling and computational simulation in predicting epidemic trends and in designing effective public health intervention strategies.

Nomenclature:

Variables (Parameters)	Description
S	Susceptible individuals
E	Exposed individuals
V	Vaccinated individuals
Q	Quarantined individuals
I_T	Infected but isolated for treatment
R	Recovered individuals
θ	Recruitment rate
τ_1	Vaccination rate
τ_2	Waning rate of vaccine
ϕ_1	Contact rate between E and S

ϕ_2	Contact rate between I_T and S
ω	Natural death rate
α_4	Rate at which the quarantined becomes susceptible
α_2	Quarantine rate of exposed
α_1	Rate at which infected are isolated for treatment
α_3	Rate at which the quarantined are isolated are treatment
γ_1	Recovery rate due to treatment
γ_2	Rate at which the vaccinated are removed
σ	COVID-19 induced death rate
γ_3	Rate at which the recovered becomes susceptible

III Solution of the non-linear initial value problem using the HomotopyPerturbation Method (HPM):

To find the solution of equation (2.1),(2.2),(2.3),(2.4),(2.5),(2.6) we construct the Homotopy as follows

$$(1-p)\left(\frac{dS}{dt}-\theta+\tau_1 S+\omega S\right)+$$
$$p\left(\frac{dS}{dt}-\theta+\tau_1 S+\omega S+\phi_1 ES+\phi_2 I_T S-\alpha_4 Q-\gamma_3 R+\tau_2 V\right)=0 \quad (3.10)$$

$$(1-p)\left(\frac{dE}{dt}+\alpha_1 E+\alpha_2 E+\omega E\right)+p\left(\frac{dE}{dt}+\alpha_1 E+\alpha_2 E+\omega E-\phi_1 ES-\phi_2 I_T S\right)=0 \quad (3.11)$$

$$(1-p)\left(\frac{dV}{dt}+\tau_2 V+\gamma_2 V+\omega V\right)+p\left(\frac{dV}{dt}+\tau_2 V+\gamma_2 V+\omega V-\tau_1 S\right)=0 \quad (3.12)$$

$$(1-p)\left(\frac{dQ}{dt}+\alpha_3 Q+\alpha_4 Q+\omega Q\right)+p\left(\frac{dQ}{dt}+\alpha_3 Q+\alpha_4 Q+\omega Q-\alpha_2 E\right)=0 \quad (3.13)$$

$$(1-p)\left(\frac{dI_T}{dt}+\gamma_1 I_T+\delta I_T+\omega I_T\right)+p\left(\frac{dI_T}{dt}+\gamma_1 I_T+\delta I_T+\omega I_T-\alpha_1 E-\alpha_3 Q\right)=0 \quad (3.14)$$

$$(1-p)\left(\frac{dR}{dt}+\gamma_3 R+\omega R\right)+p\left(\frac{dR}{dt}+\gamma_3 R+\omega R-\gamma_1 I_T-\gamma_2 V\right)=0 \quad (3.15)$$

Supposing the approximate solutions of equation (2.1-2.6) have the form

$$S=S_0+S_1 p+S_2 p^2+\cdots \quad (3.16)$$
$$E=E_0+E_1 p+E_2 p^2+\cdots \quad (3.17)$$
$$V=V_0+V_1 p+V_2 p^2+\cdots \quad (3.18)$$
$$Q=Q_0+Q_1 p+Q_2 p^2+\cdots \quad (3.19)$$
$$I_T=I_{T_0}+I_{T_1} p+I_{T_2} p^2+\cdots \quad (3.20)$$
$$R=R_0+R_1 p+R_2 p^2+\cdots \quad (3.21)$$

Substituting the equation (3.16-3.21) respectively into equation (3.10-3.15)

$$(1-p)\left[\frac{d(S_0+S_1p+S_2p^2+\cdots)}{dt}-\theta+\tau_1(S_0+S_1p+S_2p^2+\cdots)+\omega(S_0+S_1p+S_2p^2+\cdots)\right]+p\left[\frac{d(S_0+S_1p+S_2p^2+\cdots)}{dt}-\theta+\tau_1(S_0+S_1p+S_2p^2+\cdots)+\omega(S_0+S_1p+S_2p^2+\cdots)+\phi_1(E_0+E_1p+E_2p^2+\cdots)(S_0+S_1p+S_2p^2+\cdots)+\phi_2(I_{T_0}+I_{T_1}p+I_{T_2}p^2+\cdots)(S_0+S_1p+S_2p^2+\cdots)-\alpha_4(Q_0+Q_1p+Q_2p^2+\cdots)-\gamma_3(R_0+R_1p+R_2p^2+\cdots)+\tau_2(V_0+V_1p+V_2p^2+\cdots)\right]=0 \quad (3.22)$$

$$(1-p)\left[\frac{d(E_0+E_1p+E_2p^2+\cdots)}{dt}+\alpha_1(E_0+E_1p+E_2p^2+\cdots)+\alpha_2(E_0+E_1p+E_2p^2+\cdots)+\omega(E_0+E_1p+E_2p^2+\cdots)\right]+p\left[\frac{d(E_0+E_1p+E_2p^2+\cdots)}{dt}+\alpha_1(E_0+E_1p+E_2p^2+\cdots)+\alpha_2(E_0+E_1p+E_2p^2+\cdots)+\omega(E_0+E_1p+E_2p^2+\cdots)-\phi_1(E_0+E_1p+E_2p^2+\cdots)(S_0+S_1p+S_2p^2+\cdots)-\phi_2(I_{T_0}+I_{T_1}p+I_{T_2}p^2+\cdots)(S_0+S_1p+S_2p^2+\cdots)\right]=0 \quad (3.23)$$

$$(1-p)\left[\frac{d(V_0+V_1p+V_2p^2+\cdots)}{dt}+\tau_2(V_0+V_1p+V_2p^2+\cdots)+\gamma_2(V_0+V_1p+V_2p^2+\cdots)+\omega(V_0+V_1p+V_2p^2+\cdots)\right]+p\left[\frac{d(V_0+V_1p+V_2p^2+\cdots)}{dt}+\tau_2(V_0+V_1p+V_2p^2+\cdots)+\gamma_2(V_0+V_1p+V_2p^2+\cdots)+\omega(V_0+V_1p+V_2p^2+\cdots)-\tau_1(S_0+S_1p+S_2p^2+\cdots)\right]=0 \quad (3.24)$$

$$(1-p)\left[\frac{d(Q_0+Q_1p+Q_2p^2+\cdots)}{dt}+\alpha_3(Q_0+Q_1p+Q_2p^2+\cdots)+\alpha_4(Q_0+Q_1p+Q_2p^2+\cdots)+\omega(Q_0+Q_1p+Q_2p^2+\cdots)\right]+p\left[\frac{d(Q_0+Q_1p+Q_2p^2+\cdots)}{dt}+\alpha_3(Q_0+Q_1p+Q_2p^2+\cdots)+\alpha_4(Q_0+Q_1p+Q_2p^2+\cdots)+\omega(Q_0+Q_1p+Q_2p^2+\cdots)-\alpha_2(E_0+E_1p+E_2p^2+\cdots)\right]=0 \quad (3.25)$$

$$(1-p)\left[\frac{d(I_{T_0}+I_{T_1}p+I_{T_2}p^2+\cdots)}{dt}+\gamma_1(I_{T_0}+I_{T_1}p+I_{T_2}p^2+\cdots)+\delta(I_{T_0}+I_{T_1}p+I_{T_2}p^2+\cdots)+\omega(I_{T_0}+I_{T_1}p+I_{T_2}p^2+\cdots)\right]+p\left[\frac{d(I_{T_0}+I_{T_1}p+I_{T_2}p^2+\cdots)}{dt}+\gamma_1(I_{T_0}+I_{T_1}p+I_{T_2}p^2+\cdots)+\delta(I_{T_0}+I_{T_1}p+I_{T_2}p^2+\cdots)+\omega(I_{T_0}+I_{T_1}p+I_{T_2}p^2+\cdots)-\alpha_1(E_0+E_1p+E_2p^2+\cdots)-\alpha_3(Q_0+Q_1p+Q_2p^2+\cdots)\right]=0 \quad (3.26)$$

$$(1-p)\left[\frac{d(R_0+R_1p+R_2p^2+\cdots)}{dt}+\gamma_3(R_0+R_1p+R_2p^2+\cdots)+\omega(R_0+R_1p+R_2p^2+\cdots)\right]+p\left[\frac{d(R_0+R_1p+R_2p^2+\cdots)}{dt}+\gamma_3(R_0+R_1p+R_2p^2+\cdots)+\omega(R_0+R_1p+R_2p^2+\cdots)-\gamma_1(I_{T_0}+I_{T_1}p+I_{T_2}p^2+\cdots)-\gamma_2(V_0+V_1p+V_2p^2+\cdots)\right]=0$$

Equating the terms of equation (3.22-3.27) with the identical powers of p, we obtain

$$p^0:\frac{dS_0}{dt}+\tau_1S_0+\omega S_0-\theta=0 \quad (3.28)$$

$$p^0:\frac{dE_0}{dt}+\alpha_1E_0+\alpha_2E_0+\omega E_0=0 \quad (3.29)$$

$$p^0:\frac{dV_0}{dt}+\tau_2V_0+\gamma_2V_0+\omega V_0=0 \quad (3.30)$$

$$p^0: \frac{dQ_0}{dt} + \alpha_3 Q_0 + \alpha_4 Q_0 + \omega Q_0 = 0 \quad (3.31)$$

$$p^0: \frac{dI_{T_0}}{dt} + \gamma_1 I_{T_0} + \delta I_{T_0} + \omega I_{T_0} = 0 \quad (3.32)$$

$$p^0: \frac{dR_0}{dt} + \gamma_3 R_0 + \omega R_0 = 0 \quad (3.33)$$

$$p^1: \frac{dS_1}{dt} + \tau_1 S_1 + \omega S_1 + \phi_1 E_0 S_0 + \phi_2 I_{T_0} S_0 - \alpha_4 Q_0 - \gamma_3 R_0 = 0 \quad (3.34)$$

$$p^1: \frac{dE_1}{dt} + \alpha_1 E_1 + \alpha_2 E_1 + \omega E_1 - \phi_1 E_0 S_0 - \phi_2 I_{T_0} S_0 = 0 \quad (3.35)$$

$$p^1: \frac{dV_1}{dt} + \tau_2 V_1 + \gamma_2 V_1 + \omega V_1 - \tau_1 S_0 = 0 \quad (3.36)$$

$$p^1: \frac{dQ_1}{dt} + \alpha_3 Q_1 + \alpha_4 Q_1 + \omega Q_1 - \alpha_2 E_0 = 0 \quad (3.37)$$

$$p^1: \frac{dI_{T_1}}{dt} + \gamma_1 I_{T_1} + \delta I_{T_1} + \omega I_{T_1} - \alpha_1 E_0 - \alpha_3 Q_0 = 0 \quad (3.38)$$

$$p^1: \frac{dR_1}{dt} + \gamma_3 R_1 + \omega R_1 - \gamma_1 I_{T_0} - \gamma_2 V_0 = 0 \quad (3.39)$$

The explicit solution for the susceptible individuals S(t) is given by:

$$S = \frac{\theta}{\tau_1+\omega} + S(0)e^{-(\tau_1+\omega)t} - \frac{\theta e^{-(\tau_1+\omega)t}}{\tau_1+\omega} + \frac{\alpha_4 Q(0)e^{-(\tau_1+\omega)t}}{(\alpha_3+\alpha_4-\tau_1)} - \frac{\alpha_4 Q(0)e^{-(\alpha_3+\alpha_4+\omega)t}}{(\tau_3+\gamma_4-\tau_1)} + \frac{\tau_2 V(0)e^{-(\tau_1+\omega)t}}{(\tau_2+\gamma_2-\tau_1)} - \frac{\tau_2 V(0)e^{-(\tau_2+\gamma_2+\omega)t}}{(\tau_2+\gamma_2-\tau_1)} + \frac{\gamma_3 R(0)e^{-(\tau_1+\omega)t}}{(\gamma_3-\tau_1)} - \frac{\gamma_3 R(0)e^{-(\gamma_3+\omega)t}}{(\gamma_3-\tau_1)} - \frac{\phi_1\theta E(0)e^{-(\tau_1+\omega)t}}{(\tau_1+\omega)(\alpha_1+\alpha_2-\tau_1)} + \frac{\phi_1\theta E(0)e^{-(\alpha_1+\alpha_2+\omega)t}}{(\tau_1+\omega)(\alpha_1+\alpha_2-\tau_1)} - \frac{\phi_2\theta I_T(0)e^{-(\tau_1+\omega)t}}{(\tau_1+\omega)(\gamma_1+\delta-\tau_1)} + \frac{\phi_2\theta I_T(0)e^{-(\gamma_1+\delta+\omega)t}}{(\tau_1+\omega)(\gamma_1+\delta-\tau_1)} - \frac{\phi_1 E(0)S(0)e^{-(\tau_1+\omega)t}}{(\alpha_1+\alpha_2+\omega)} + \frac{\phi_1 E(0)S(0)e^{-(\alpha_1+\alpha_2+\omega)t}}{(\alpha_1+\alpha_2+\omega)} + \frac{\phi_1\theta E(0)e^{-(\tau_1+\omega)t}}{(\tau_1+\omega)(\alpha_1+\alpha_2+\omega)} - \frac{\phi_1\theta E(0)e^{-(\alpha_1+\alpha_2+\omega)t}}{(\tau_1+\omega)(\alpha_1+\alpha_2+\omega)} - \frac{\phi_2\theta I_T(0)S(0)e^{-(\tau_1+\omega)t}}{(\gamma_1+\delta+\omega)} + \frac{\phi_2\theta I_T(0)S(0)e^{-(\gamma_1+\delta+\omega)t}}{(\gamma_1+\delta+\omega)} + \frac{\phi_2\theta I_T(0)e^{-(\tau_1+\omega)t}}{(\tau_1+\omega)(\gamma_1+\delta+\omega)} - \frac{\phi_2\theta I_T(0)e^{-(\gamma_1+\delta+\omega)t}}{(\tau_1+\omega)(\gamma_1+\delta+\omega)} \quad (3.40)$$

The explicit solution for the exposed individuals E(t) is given by:

$$E = E(0)e^{-(\alpha_1+\alpha_2+\omega)t} + \frac{\phi_1\theta E(0)te^{-(\alpha_1+\alpha_2+\omega)t}}{(\tau_1+\omega)} + \frac{\phi_1 E(0)S(0)e^{-(\alpha_1+\alpha_2+\omega)t}}{(\tau_1+\omega)} - \frac{\phi_1 E(0)S(0)e^{-(\tau_1+\alpha_1+\alpha_2+2\omega)t}}{(\tau_1+\omega)} - \frac{\phi_1\theta E(0)te^{-(\alpha_1+\alpha_2+\omega)t}}{(\tau_1+\omega)(\tau_1+\omega)} + \frac{\phi_1\theta E(0)te^{-(\tau_1+\alpha_1+\alpha_2+2\omega)t}}{(\tau_1+\omega)(\tau_1+\omega)} + \frac{\phi_2\theta I_T(0)e^{-(\alpha_1+\alpha_2+\omega)t}}{(\tau_1+\omega)(\gamma_1+\delta-\alpha_1-\alpha_2)} - \frac{\phi_2\theta I_T(0)e^{-(\gamma_1+\delta+\omega)t}}{(\tau_1+\omega)(\gamma_1+\delta-\alpha_1-\alpha_2)} + \frac{\phi_2 I_T(0)S(0)e^{-(\alpha_1+\alpha_2+\omega)t}}{(\gamma_1+\delta+\tau_1-\alpha_1-\alpha_2)} - \frac{\phi_2 I_T(0)S(0)e^{-(\gamma_1+\delta+\tau_1+\omega)t}}{(\gamma_1+\delta+\tau_1-\alpha_1-\alpha_2)} - \frac{\phi_2\theta I_T(0)e^{-(\alpha_1+\alpha_2+\omega)t}}{(\tau_1+\omega)(\gamma_1+\delta+\tau_1-\alpha_1-\alpha_2)} + \frac{\phi_2\theta I_T(0)e^{-(\gamma_1+\delta+\tau_1+\omega)t}}{(\tau_1+\omega)(\gamma_1+\delta+\tau_1-\alpha_1-\alpha_2)} \quad (3.41)$$

he explicit solution for the vaccinated individuals V(t) is given by:

$$V = V(0)e^{-(\tau_2+\gamma_2+\omega)t} + \frac{\tau_1\theta}{(\tau_1+\omega)(\tau_2+\gamma_2+\omega)} - \frac{\tau_1\theta e^{-(\tau_2+\gamma_2+\omega)t}}{(\tau_1+\omega)(\tau_2+\gamma_2+\omega)} + \frac{\tau_1 S(0)e^{-(\tau_1+\omega)t}}{(\tau_2+\gamma_2-\tau_1)} - \frac{\tau_1 S(0)e^{-(\tau_2+\gamma_2+\omega)t}}{(\tau_2+\gamma_2-\tau_1)} - \frac{\tau_1\theta e^{-(\tau_1+\omega)t}}{(\tau_1+\omega)(\tau_2+\gamma_2-\tau_1)} + \frac{\tau_1\theta e^{-(\tau_2+\gamma_2+\omega)t}}{(\tau_1+\omega)(\tau_2+\gamma_2-\tau_1)} \quad (3.42)$$

The explicit solution for the quarantined individuals Q(t) is given by:

$$Q = Q(0)e^{-(\alpha_3+\alpha_4+\omega)t} + \frac{\alpha_2 E(0)e^{-(\alpha_1+\alpha_2+\omega)t}}{(\alpha_3+\alpha_4-\alpha_1-\alpha_2)} - \frac{\alpha_2 E(0)e^{-(\alpha_3+\alpha_4+\omega)t}}{(\alpha_3+\alpha_4-\alpha_1-\alpha_2)} \quad (3.43)$$

The explicit solution for the infected isolated individuals $I_T(t)$ is given by:

$$I_T = I_T(0)e^{-(\gamma_1+\delta+\omega)t} + \frac{\alpha_1 E(0)e^{-(\alpha_1+\alpha_2+\omega)t}}{(\gamma_1+\delta-\alpha_1-\alpha_2)} - \frac{\alpha_1 E(0)e^{-(\gamma_1+\delta+\omega)t}}{(\gamma_1+\delta-\alpha_1-\alpha_2)} + \frac{\alpha_3 Q(0)e^{-(\alpha_3+\alpha_4+\omega)t}}{(\gamma_1+\delta-\alpha_3-\alpha_4)} - \frac{\alpha_3 Q(0)e^{-(\gamma_1+\delta+\omega)t}}{(\gamma_1+\delta-\alpha_3-\alpha_4)} \quad (3.44)$$

The explicit solution for the recovered individuals R(t) is given by:

$$R = R(0)e^{-(\gamma_3+\omega)t} + \frac{\gamma_1 I_T(0)e^{-(\gamma_1+\delta+\omega)t}}{(\gamma_3-\gamma_1-\delta)} - \frac{\gamma_1 I_T(0)e^{-(\gamma_3+\omega)t}}{(\gamma_3-\gamma_1-\delta)} + \frac{\gamma_2 V(0)e^{-(\tau_2+\gamma_2+\omega)t}}{(\gamma_3-\tau_1-\gamma_2)} - \frac{\gamma_2 V(0)e^{-(\gamma_3+\omega)t}}{(\gamma_3-\tau_1-\gamma_2)} \quad (3.45)$$

Numerical Simulation:

The system of non-linear differential equations (2.1)-(2.6) is solved numerically using the Homotopy Perturbation Methods (HPM). This method provides an approximate analytical solution, which is further validated through numerical simulation.

For the purpose of simulation, the following initial conditions are considered:

S(0) = 1000, E(0) = 500, V(0) = 300, Q(0) = 200, $I_T(0) = 0$, R(0) = 0

The parameter values used in the simulation are listed below:

Parameters	Values
θ	400
τ_1	0.1
τ_2	0.001
ϕ_1	0.000018
ϕ_2	0.000017
ω	0.0096
α_4	0.0001
α_2	0.05

α_1	0.04
α_3	0.01
γ_1	0.16979
γ_2	0.16979
σ	0.03275
γ_3	0.23

MATLAB software is used to simulate the system numerically. The results are obtained using standard numerical solvers and are represented graphically to understand the behavior of different compartments over time.

IV. RESULTS AND DISCUSSION

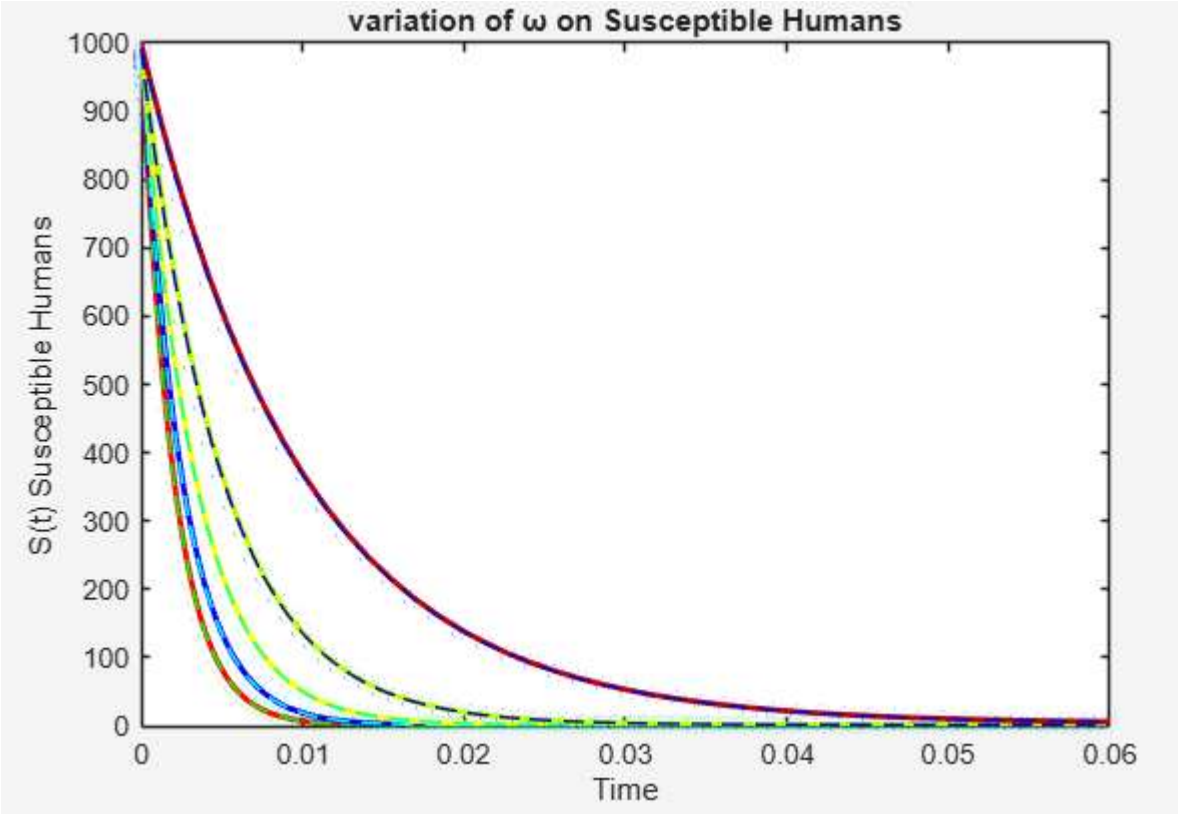


Figure 1

The graph illustrates the variation of susceptible humans S(t) with respect to time for different values of the deathω = 100, 200, 300, 400, 500.

From the figure 1, it is observed that the number of susceptible individuals decreases rapidly as time increases. For lower natural death rateω = 100, the decline in the susceptible population is slower, whereas for higher natural death rateω = 500, the susceptible population decreases very rapidly within a short period of time. All curves start from the same initial population but diverge significantly as time progresses.

Thus, it is concluded that an increase in the natural death rate ω accelerates the reduction of susceptible humans, showing that it has a strong influence on the system dynamics.

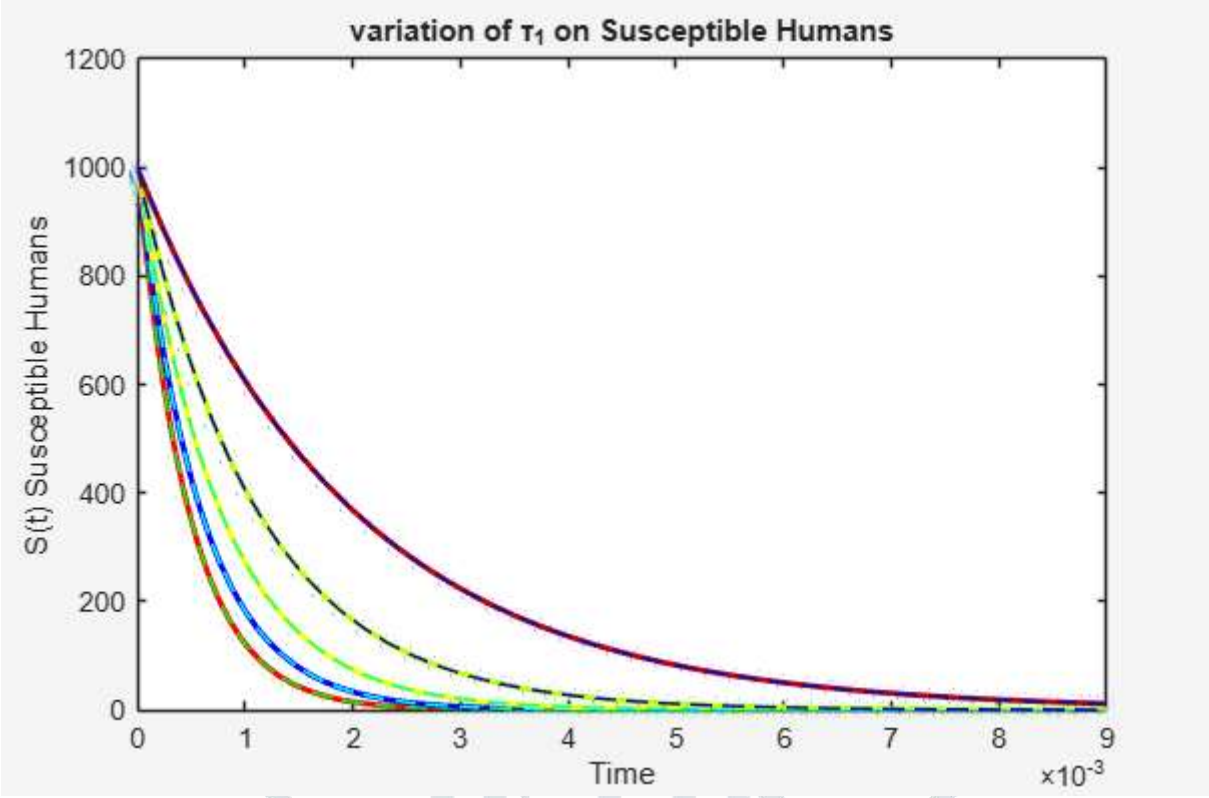


Figure 2

The graph illustrates the variation of susceptible humans S(t) with respect to time for different values of the vaccination rate τ_1 = 100, 500, 900, 1300, 1700.

From the figure 2, it is observed that the number of susceptible individuals decreases rapidly as time increases. For lower vaccination rate τ_1= 100, the decline in the susceptible population is slower, whereas for higher vaccination rate τ_1= 1700, the susceptible population decreases very rapidly within a short period of time. All curves start from the same initial population but diverge significantly as time progresses.

Thus, it is concluded that an increase in the vaccination rate τ_1 accelerates the reduction of susceptible humans, showing that it has a strong influence on the system dynamics.

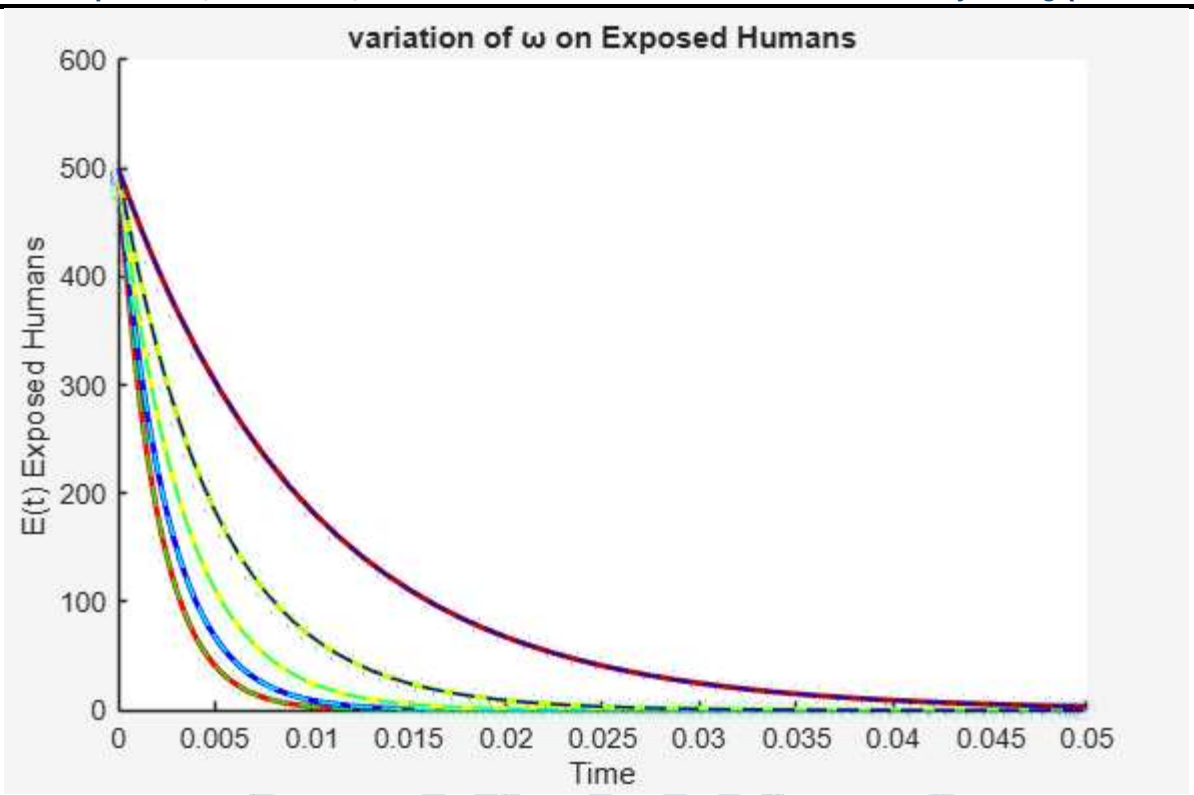


Figure 3

The graph illustrates the variation of exposed humans E(t) with respect to time for different values of the natural death rate ω = 100, 200, 300, 400, 500.

From the figure 3, it is observed that the number of exposed individuals decreases rapidly as time increases. For lower natural death rate ω = 100, the decline in the exposed population is slower, whereas for higher natural death rate ω = 500, the exposed population decreases very rapidly within a short period of time. All curves start from the same initial population but diverge significantly as time progresses.

Thus, it is concluded that an increase in the natural death rate ω accelerates the reduction of exposed humans, showing that it has a strong influence on the system dynamics.

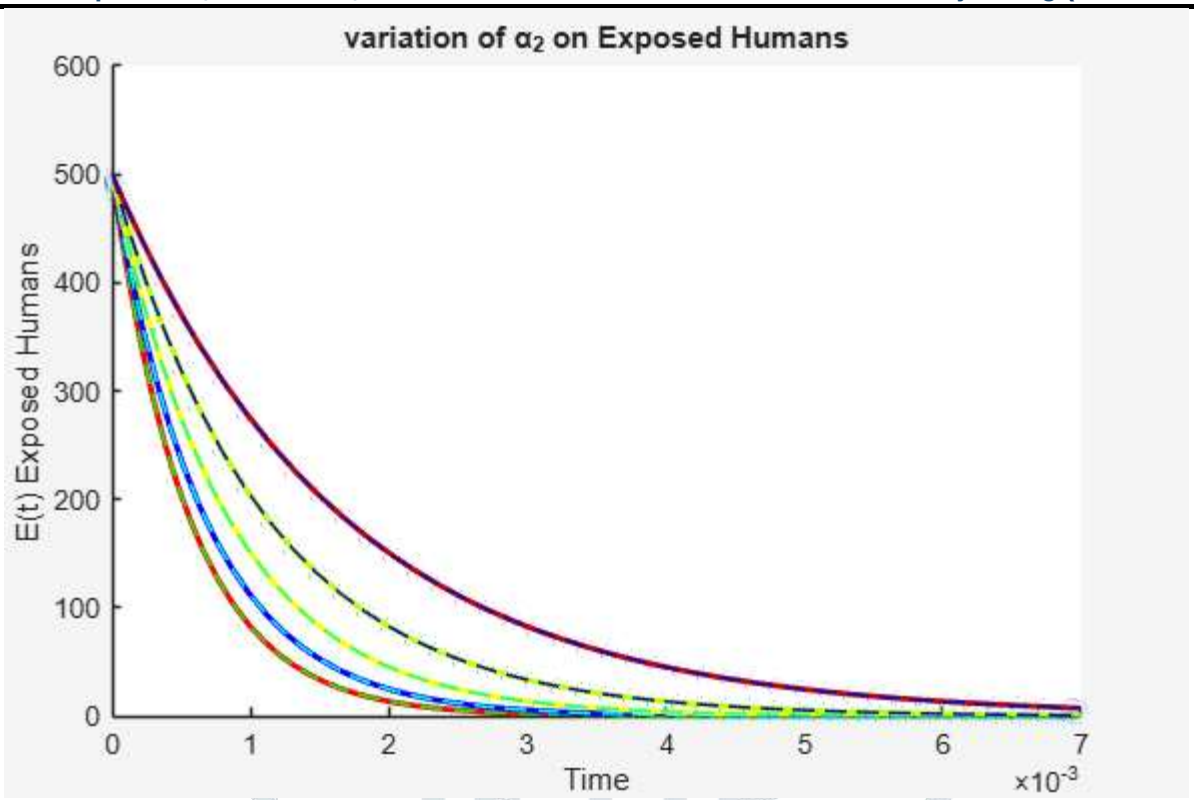


Figure 4

The graph illustrates the variation of exposed humans E(t) with respect to time for different values of the quarantine rate of exposed individuals α_2= 100, 400, 700, 1000, 1300.

From the figure 4, it is observed that the number of exposed individuals decreases rapidly as time increases. For lower quarantine rate α_2= 100, the decline in the exposed population is slower, whereas for higher quarantine rate α_2 = 1300, the exposed population decreases very rapidly within a short period of time. All curves start from the same initial population but diverge significantly as time progresses.

Thus, it is concluded that an increase in the quarantine rate $\alpha_2$accelerates the reduction of exposed humans, showing that it has a strong influence on the system dynamics.

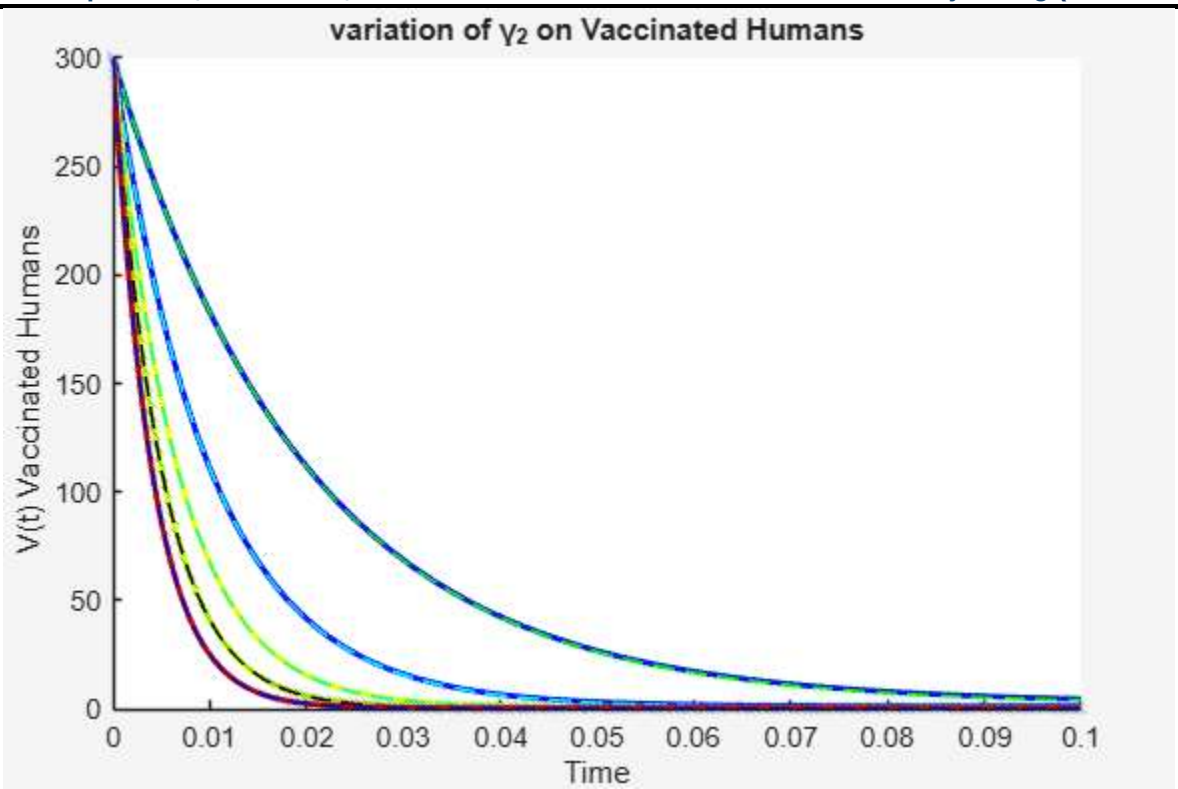


Figure 5

The graph illustrates the variation of vaccinated humans V(t) with respect to time for different values of the removal rate γ_2 = 50, 100, 150, 200, 250.

From the figure 5, it is observed that the number of vaccinated individuals decreases rapidly as time increases. For lower removal rate γ_2= 50, the decline in the vaccinated population is slower, whereas for higher removal rate γ_2= 250, the vaccinated population decreases very rapidly within a short period of time. All curves start from the same initial population but diverge significantly as time progresses.

Thus, it is concluded that an increase in the removal rate $\gamma_2$accelerates the reduction of vaccinated humans, showing that it has a strong influence on the system dynamics.

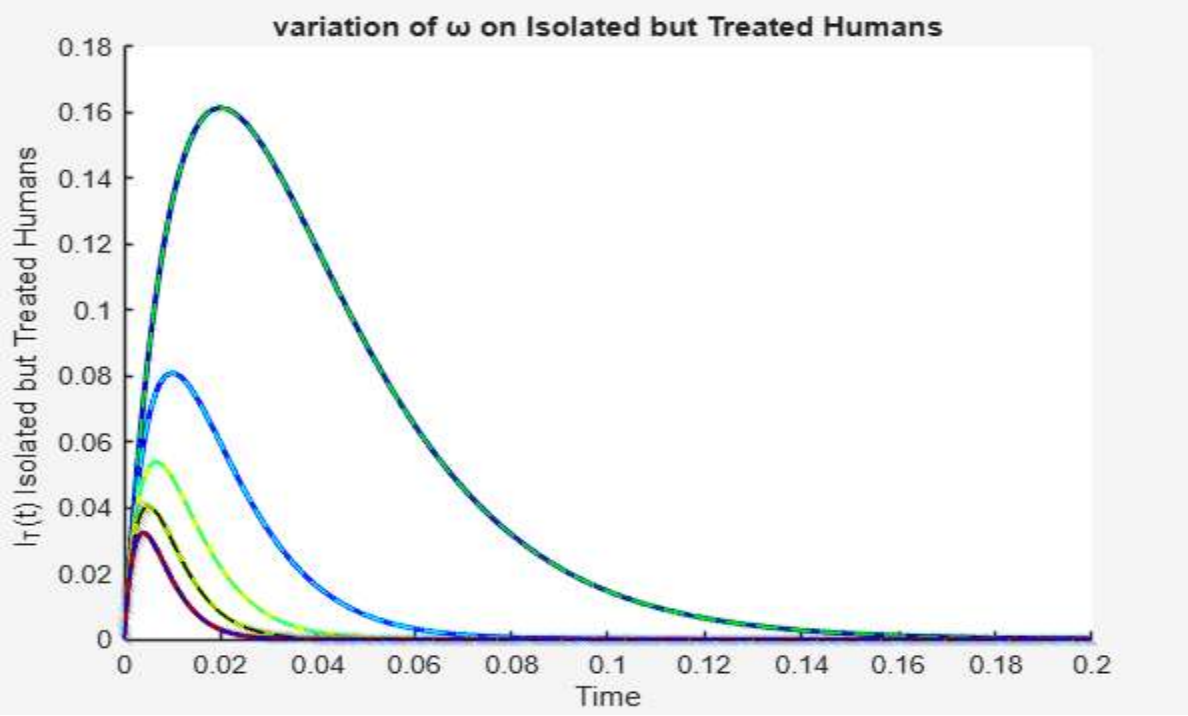


Figure 6

The graph illustrates the variation of isolated but treated humans $I_T(t)$ with respect to time for different values of the natural death rate ω = 50, 100, 150, 200, 250.

From the figure 6, it is observed that the number of isolated but treated individuals initially increases and then decreases rapidly as time increases. For lower natural death rate ω = 50, the decline in the treated population is slower and reaches a higher peak, whereas for higher natural death rate ω = 250, the population decreases very rapidly and stay at a much lower level. All curves follow a similar trend but diverge significantly as the death rate increases.

Thus, it is concluded that an increase in the natural death rate ω accelerates the reduction of isolated but treated humans, showing that it has a strong influence on the system dynamics.

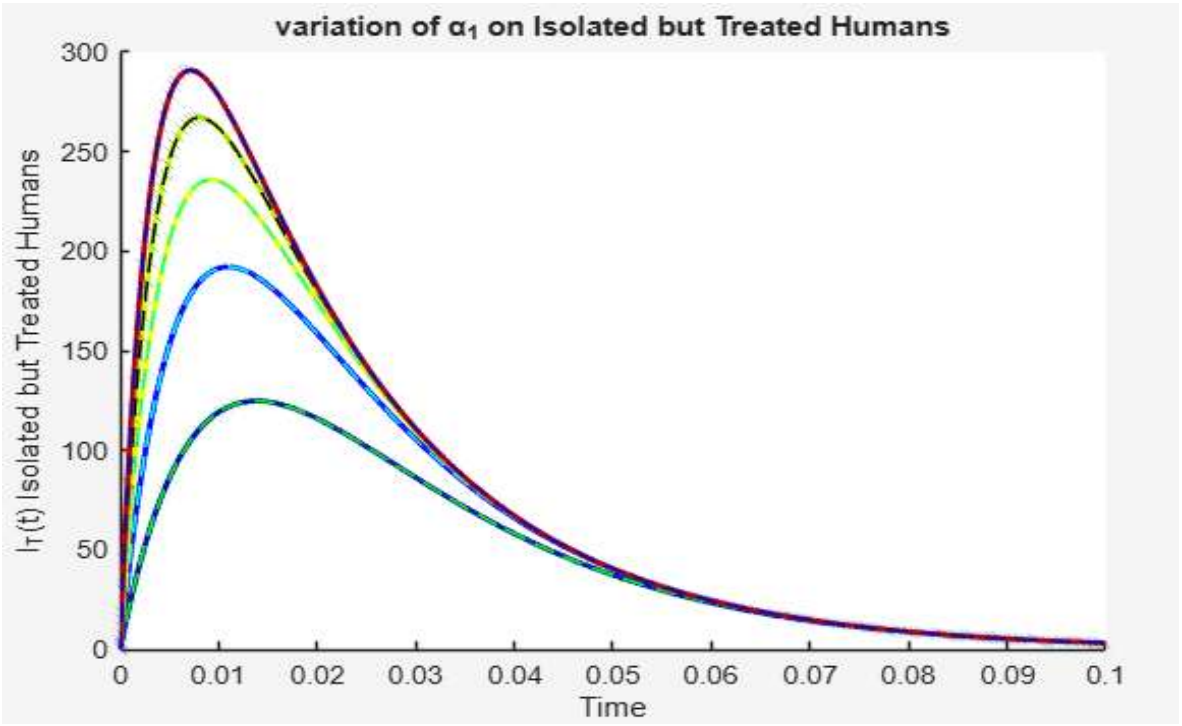


Figure 7

The graph illustrates the variation of isolated but treated humans $I_T(t)$ with respect to time for different values of the rate at which infected are isolated for treatment α_1 = 50, 100, 150, 200, 250.

From the figure 7, it is observed that the number of isolated but treated individuals initially increases rapidly and then decreases as time progresses. For lower treatment rate α_1 = 50, the peak of the treated population is lower, whereas for higher treatment rate α_1 = 250, the population increases very rapidly and reaches a higher peak within a short period of time. All curves start from zero and diverge significantly before converging as time progresses.

Thus, it is concluded that an increase in the isolation and treatment rate α_1 accelerates the growth of isolated but treated humans, showing that it has a strong influence on the system dynamics.

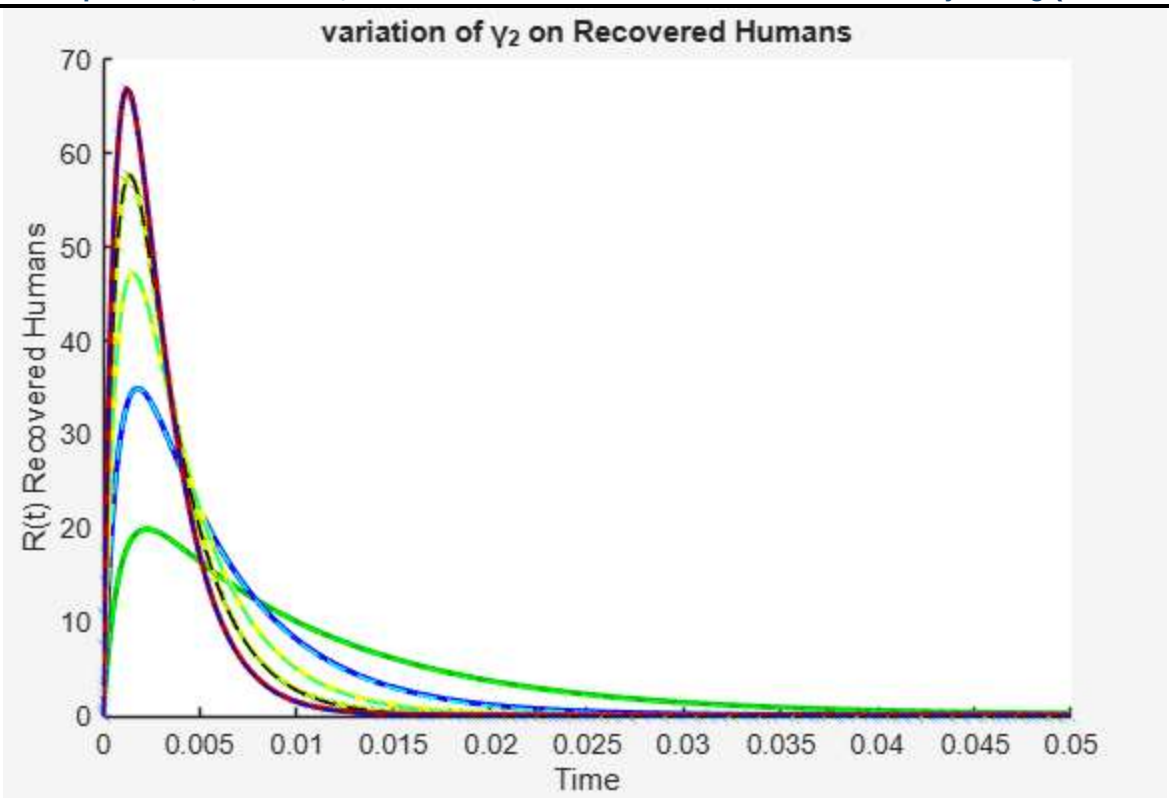


Figure 8

The graph illustrates the variation of recovered humans R(t) with respect to time for different values of the rate at which the vaccinated are removed γ_2 = 100, 200, 300, 400, 500.

From the figure 8, it is observed that the number of recovered individuals initially increases and then decreases as time progresses. For lower removal rate γ_2 = 100, the peak of the recovered population is lower and more spread out, whereas for higher removal rate γ_2= 500, the recovered population increases very rapidly and reaches a higher peak within a very short period of time. All curves start from zero and diverge significantly before converging back to a steady state.

Thus, it is concluded that an increase in the rate γ_2 accelerates the growth and peak of recovered humans, showing that it has a strong influence on the system dynamics.

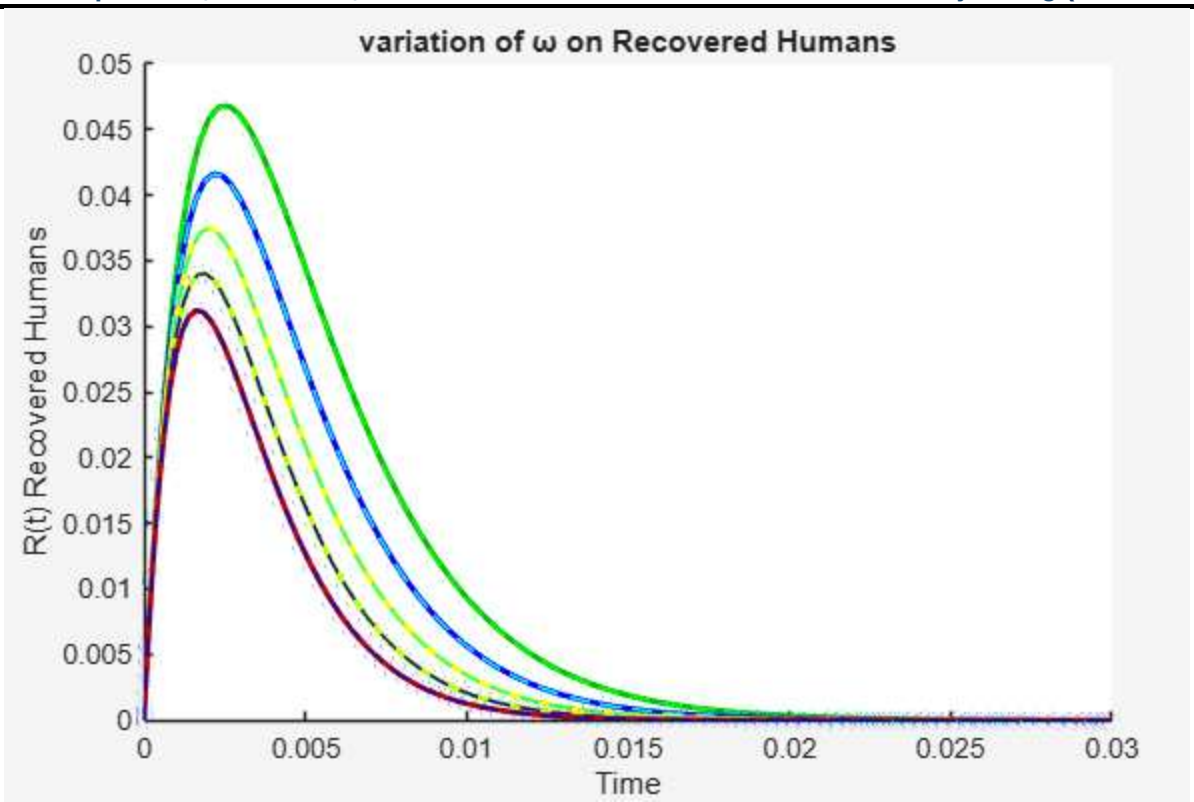


Figure 9

The graph illustrates the variation of recovered humans R(t) with respect to time for different values of the natural death rate ω = 400, 450, 500, 550, 600.

From the figure 9, it is observed that the number of recovered individuals initially increases and then decreases as time progresses. For lower natural death rate ω = 400, the peak of the recovered population is higher, whereas for higher natural death rate ω = 600, the recovered population reaches a much lower peak and decreases rapidly. All curves follow a similar trajectory but diverge significantly based on the death rate.

Thus, it is concluded that an increase in the natural death rate ω accelerates the reduction and lowers the peak of recovered humans, showing that it has a strong influence on the system dynamics.

Conclusion:

In this work, a mathematical model has been developed to study the transmission dynamics of the disease system. The system of nonlinear differential equations was solved numerically to analyze the behavior of different compartments, namely susceptible S(t), vaccinated V(t), quarantined Q(t), and isolated but treated $I_T(t)$. The results provide a clear understanding of how the disease spreads and how it can be controlled under varying conditions.

The analysis shows that the model is highly influenced by key parameters such as the natural death rate ω, vaccination removal rate γ_2, waning immunity rate τ_2, and treatment rates α_1,α_3,α_4. An increase in the death rate and vaccination removal rate leads to a rapid decline in the susceptible and vaccinated populations. Similarly, higher waning rates reduce the long-term effectiveness of vaccination.

Moreover, the treatment and isolation rates play a significant role in reducing the spread of infection. Higher values of treatment parameters help in lowering the peak of infected and quarantined populations, indicating better disease control. Thus, the study concludes that proper vaccination strategies, along with effective treatment and isolation measures, are essential to control the spread of the disease. The model provides useful insights for understanding and managing infectious diseases.

REFERENCES

[1] World Health Organization, *Report of the WHO-China joint mission on coronavirus disease 2019 (COVID-19)*, 2020.https://www.who.int/docs/sefaultsource/coronaviruse/who-china-joint-mission-on-covid-19-final-report.pdf

[2] World/Countries/Pakistan, *Total Coronavirus Cases in Pakistan*, Available online: https://www.worldometers.info/coronavirus/country/pakistan/

[3] R.O.Aja, W.Atokolo, D.Omale, G.O.Acheneje, J.Amos, A.C.Benedict,*Mathematical Analysis of COVID-19 Fractional Model Incorporating Vaccination, Quarantine and Isolation Measures 2048-3077,2025*. DOI:10.12150/juma.2025.2048

[4] S. Khajanchi, K.Sarkar, S. Banerjee, *Modeling the dynamics of COVID-19 pandemic with implementation of intervention strategies*, Eur. Phys. J. Plus 137, 1-22,2022. DOI:10.1140/epjp/s13360-022-01610-3

[5] Li T., Guo Y., *Modeling and optimal control of mutated COVID-19{Delta strain) with imperfect vaccination*, 156 (2022)

[6] Zeroual A., Harrou F., Dairi A., Sun Y., *Deep learning methods for forecasting COVID-19 time-Series data: A Comparative study*,Chaoa, Solitons and Fractals 140 (2020) 110121

[7] Arunkumar K., Kalaga D.V., Kumar C.M.S., Kawaji M., Brenza T.M., *Forecasting of COVID-19 using deep layer recurrent neural netwouks (RNNs) with gated recurrent units (GRUs) and long short-term memory (LSTM) cells*, Chaos, Solitons and Fractals1 46 (2021) 110861

[8] M.S. Ullah, M. Higazy, K.A. Kabir, *Modeling te epidemic control measures in overcoming COVID-19 outbreaks: A fractional-order derivative approach*, Chaos Solitons Fractals 155, 111636, 2022. DOI: 10.1016/j/chaos.2022.222636

[9] Remigius Okeke Aja, Mathematical Analysis of COVID-19 Fractional model incorporating vaccination, Quarantine and Isolation measures, Journal of Nonllinear modeling and analysis,(2025)2048-2077.

[10] Tingting Li, Youming Guo, Modeling and optimal control of mutated acovid-19(Delta strain) with imperfect vaccination, Chaos,solitons and Fractals 156(2022)111825.